

# PROCEEDINGS OF SPIE

[SPIDigitalLibrary.org/conference-proceedings-of-spie](https://spiedigitallibrary.org/conference-proceedings-of-spie)

## Deployment of beam alignment hardware at the Magdalena Ridge Observatory Interferometer

Luis, James J., Buscher, David, Dahl, Chuck, Dooley, Jonathan, Farris, Allen, et al.

James J. D. Luis, David F. Buscher, Chuck Dahl, Jonathan F. Dooley, Allen Farris, Christopher A. Haniff, E. Robert Ligon, Siavash Norouzi, Xiaowei Sun, John S. Young, "Deployment of beam alignment hardware at the Magdalena Ridge Observatory Interferometer," Proc. SPIE 11446, Optical and Infrared Interferometry and Imaging VII, 1144628 (13 December 2020); doi: 10.1117/12.2562863

**SPIE.**

Event: SPIE Astronomical Telescopes + Instrumentation, 2020, Online Only

# Deployment of beam alignment hardware at the Magdalena Ridge Observatory Interferometer

James J. D. Luis<sup>a</sup>, David F. Buscher<sup>a</sup>, Chuck Dahl<sup>b</sup>, Jonathan F. Dooley<sup>b</sup>, Allen Farris<sup>b</sup>, Christopher A. Haniff<sup>a</sup>, E. Robert Ligon<sup>b</sup>, Siavash Norouzi<sup>b</sup>, Xiaowei Sun<sup>a</sup>, and John S. Young<sup>a</sup>

<sup>a</sup>Cavendish Laboratory, University of Cambridge, Cambridge, United Kingdom

<sup>b</sup>Magdalena Ridge Observatory, New Mexico Institute of Mining and Technology, Socorro, New Mexico, USA

## ABSTRACT

The first unit telescope of the Magdalena Ridge Observatory Interferometer is integrated on the array and starlight has been observed in the Beam Combining Area for the first time. From the telescope, the beam travels in vacuum over a path of >50m, including a beam relay system and delay line. This feat was made possible by a prototype version of the Automated Alignment System that we are developing for minimising fringe visibility loss due to misalignment. We present results of on-site validation of UTLIS, a reference light source at the unit telescope acting as a proxy for starlight, and BEASST, a Shack-Hartmann sensor that simultaneously detects beam angle and position.

**Keywords:** Magdalena Ridge Observatory Interferometer, MROI, interferometry, active optics, Shack-Hartmann, beam alignment, automated alignment

## 1. INTRODUCTION

The Magdalena Ridge Observatory Interferometer (MROI) is an optical interferometer under development in New Mexico, USA. When finished it will harness ten relocatable 1.4m-diameter Unit Telescopes (UTs) for high angular resolution studies of targets such as active galactic nuclei (AGN) and young stellar objects at optical wavelengths (0.6  $\mu\text{m}$  to 2.4  $\mu\text{m}$ ). Figure 1 shows an impression of the completed facility.

The project aims to maximise sensitivity. We hope to reach a limiting magnitude for fringe tracking of  $m_H = 14$  to unlock a larger number of targets (eg 100 AGN) than has been inaccessible to previous generations of optical interferometers. This ambitious goal necessitates a strict error budget for the performance of MROI. One important consideration is beam alignment. Deviations from the nominal alignment degrade the signal to noise ratio of fringe visibility measurements.<sup>1</sup> We are therefore working on an Automated Alignment System (AAS) that will align all beamlines of MROI at the start of an observing night, then proceed to correct beam pointing drifts throughout the night, all with minimal human interaction.

MROI is progressing towards achieving first stellar fringes between two UTs. We had hoped to achieve this goal already, but the project has been delayed by the Covid-19 pandemic and ensuing complications which have halted on-site operations. Nevertheless, one UT is now fully integrated at the apex of the array. In late 2019, we carried out some commissioning activities that resulted in starlight being passed from the UT through to the Beam Combining Area (BCA) for the first time. This feat was achieved by the deployment of a simplified version of the AAS. This paper discusses the results of on-site testing of prototypes of the Unit Telescope Light Injection System (UTLIS), which is a light source located at the UT; and Back End Active Stabilisation of Shear and Tilt (BEASST), which is an alignment detector in the BCA. We have dubbed these prototypes UTLIS0 and BEASST0.

---

Further author information: (Send correspondence to J. J. D. Luis)  
E-mail: jjdl3@mrao.cam.ac.uk, Telephone: +44 1223 337 137

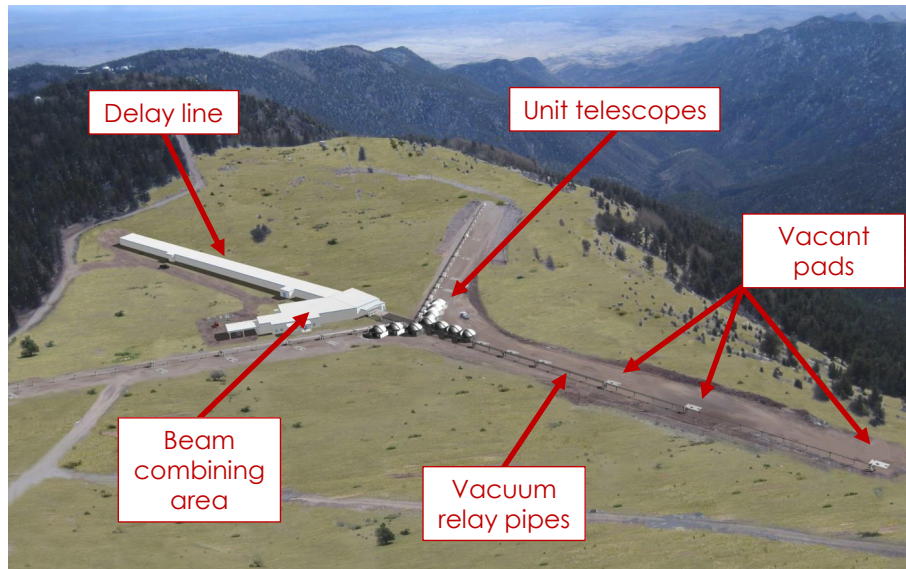


Figure 1: Artist's impression of the completed MROI in a closely packed configuration of UTs. Currently one UT is placed on a station at the array apex. The beam relay and delay line are populated with optics to deliver a beam to the BCA.

## 2. ALIGNMENT SYSTEM OVERVIEW

The AAS ensures that during observing, the 10 beams of MROI arrive on the nominal axes of the beam combiners within an angle (tilt) of 15 mas on sky and position (shear) of 1% of the pupil diameter. To understand how the alignment system fits into the beam train, it is first useful to visualise a single MROI beam train with Figure 2. It can be broken down into 3 optical axes (ellipses): the Unit Telescope (UT), Delay Line (DL) and Beam Combiners (BC). Between each of these axes is a pair of steerable mirrors (gold boxes, M4/M5 and M11/M12) that will map adjacent axes to each other. The beamline is split into two regimes of beam diameter, 95 mm (left) and 13 mm (right), resulting from a 7.3x beam compressor (BCr) in the BCA. Optics in the 95mm-space are mostly located in unstable thermal environments, so their contribution to drifts will dominate. In the 13mm-space, the error budget for tilt magnifies to 1.6 arcseconds while the term for shear becomes 130  $\mu\text{m}$ . To achieve the sensitivity goal of the interferometer, these values should not be exceeded at any time during observations.

Figure 3 folds alignment hardware into the beamline. Two light sources are injected into the beam train:

- MOB in the BCA (orange beam) - MOB (Magical Optical Box) is a combined broadband and laser source which can be injected at will to send light towards the UT and/or towards the beam combiners. During start-of-night alignment procedures it is sampled by two retractable photovoltaic quad cells, QC1 and QC3, in the vacuum beam relay that will help to align MOB to the DL axis. It also provides light for BEASST and alignment detectors in the beam combiners (not shown here).
- UTLIS at the UT (green beam) - UTLIS acts as a proxy for starlight. Injected at the dichroic splitter for the Fast Tip-Tilt correction system (FTT), it passes light to the FTT camera and towards the BCA (see Figure 5). The FTT<sup>2</sup> views stellar light and establishes a closed loop with the secondary mirror of the UT to correct atmospheric tip-tilt perturbations. The tilt of the UTLIS beam is measured by the FTT and registered as the fiducial for closed loop operation so that the stellar beam will be ejected from the UT at the same angle as the UTLIS beam. The shear, however, might be offset because the telescope pupil is fixed. The UTLIS beam propagating downstream will be viewed by QC2 in the beam relay, and BEASST.

To keep this description brief, we will not outline the start-of-night alignment procedure here, but note that once the beamline has been aligned, the UTLIS beam is registered by BEASST as a fiducial for tilt and shear.

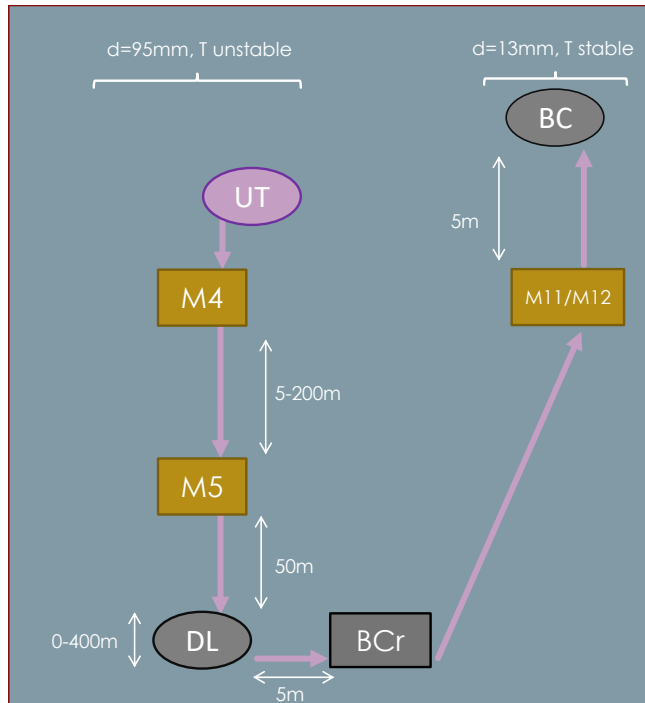


Figure 2: Schematic showing optics for a single beamline of MROI. Starlight is collected by a UT, then enters a vacuum pipe to be relayed towards the BCA by mirrors M4 and M5. The spacing between M4 and M5 increases with distance of the UT from the array apex. Before entering the BCA, the beam passes through a delay line (DL), still in vacuum, which can add up to 400 m of path length (only 200 m is possible currently). The beam exits the delay line (and vacuum) into the beam combining area. The 95 mm diameter beam is reduced to 13 mm by a 7.3x beam compressor (BCr) so that the size of optics is more manageable for beam combination. M11 and M12 are mirrors or dichroic splitters which direct the beams to the beam combiners (BC) for fringe tracking and science.

Mirrors M4 and M5 have been measured to creep by an intolerable amount as a function of temperature. If no compensation was applied after start-of-night alignment, the drifts in tilt and shear would exceed their budgets within a few minutes. The problem is worst directly after sunset as the temperature drops rapidly. The AAS will coordinate an intra-night realignment procedure to counteract such drifts. We will use localised temperature sensors (T4/T5, blue boxes) on the mirror mounts to generate a predictive model of drift. During stellar observations, realtime temperature readings will be compared against the model to forecast how much the alignment has drifted. M4 and M5 will be tilted to "blindly" compensate for the drift. Residuals from the model will need to be measured and corrected in between stellar observations, perhaps every 10 minutes. UTLIS will be switched on and viewed on BEASST. Its light will first be viewed on the FTT camera to reset the fiducial for closed loop tip-tilt correction, which calibrates out any tilt drift of UTLIS itself. At the same time, UTLIS light will be viewed on BEASST to identify the residuals and subsequently remove them.

In support of commissioning tests of the first beamline in 2019, we installed the following prototypes of the AAS:

- UTLIS0,
- QC1, QC2, QC3
- MOB0
- BEASST0

While MOB0 and the QCs were crucial for achieving good beam alignment, this paper focuses on our experiences of fielding UTLIS0 and BEASST0.

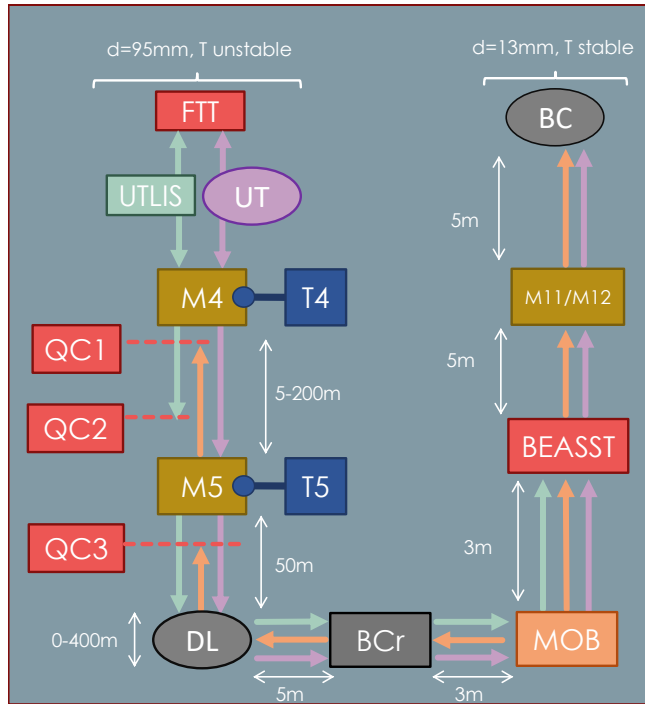


Figure 3: Schematic showing the complete set of alignment hardware embedded within a beamline. Red boxes correspond to detectors: QCs are retractable photovoltaic quad cells, BEASST is a tilt and shear detector, FTI is a tilt detector. T4/T5 are localised temperature sensors attached to mirrors M4 and M5.

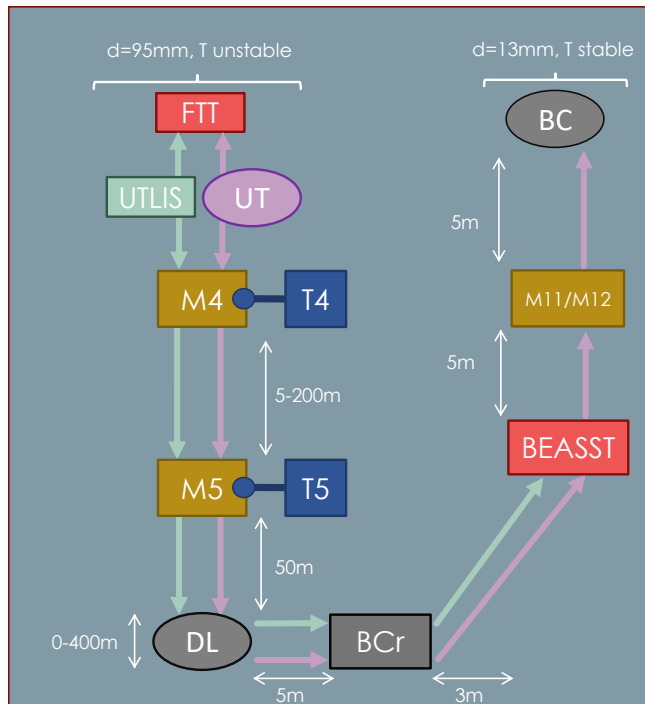


Figure 4: Schematic showing a beamline and its embedded hardware for intranight alignment compensation. Components are defined in Figures 2 and 3. The correction strategy is outlined in the main text.

### 3. UNIT TELESCOPE LIGHT SOURCE

UTLIS0 outputs a collimated beam of wavelength 830 nm as a proxy for the starlight beam. Its design was optimised for speed of delivery, and so it is assembled entirely from off-the-shelf components. Light is generated by a superluminescent diode in a remote cabinet, then transported by single mode fiber to the Nasmyth Table (NT) of the UT. Figure 5 depicts the optical layout on the NT. The light emerging from the fiber is collimated by an achromatic doublet lens (Edmund Optics 88-596,  $f=200$  mm,  $d = 75$  mm) then injected into the beam train at the FTT dichroic splitter. In reflection, the beam is passed downstream towards the beam relay, delay line and BCA. In transmission the beam passes to the FTT camera. The current splitter coating is such that 90% of intensity is reflected, while 10% is transmitted. A mirror pair enables the tilt and shear of the beam to be configured remotely with piezo-internia actuators (Thorlabs PIA13).

UTLIS0 operates at a single wavelength, but the production version will combine several wavelengths to cater for various detector sensitivities. For example, the QCs and FTT camera are most sensitive at visible wavelengths while BEASST observes between  $1.1\ \mu\text{m}$  and  $1.7\ \mu\text{m}$ . The production version of UTLIS will replace the single mode fiber of UTLIS0 with a photonic crystal fiber to ensure single mode behaviour at the chosen wavelengths.

#### 3.1 Beam diameter

The beam diameter should be as large as possible to reduce expansion due to diffraction; ideally it would be matched with the starlight beam diameter of 95 mm. However, for UTs located on the West Arm of the interferometer, Mirror M4 is placed on the Nasmyth Table of the UT rather than inside the vacuum beam relay pipes. In this configuration, M4 is positioned closely with respect to UTLIS, imposing an upper limit on its beam diameter to avoid obscuration by the M4 mount. For UTLIS0, we aimed for a 50mm diameter as a tradeoff between these two considerations. Laboratory testing revealed that, at 32.7 mm, the  $1/e^2$  diameter was narrower than the fiber's numerical aperture would suggest. It turns out that a more accurate estimate comes from Gaussian beam propagation, where the waist is the mode field diameter of the fiber.

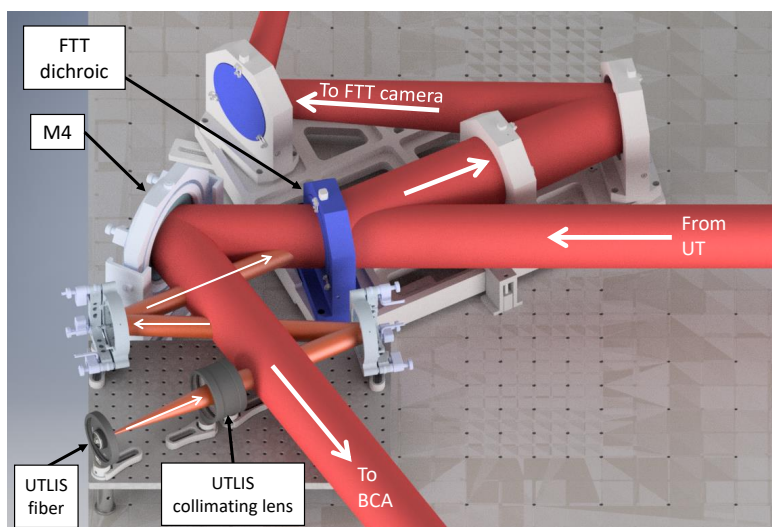
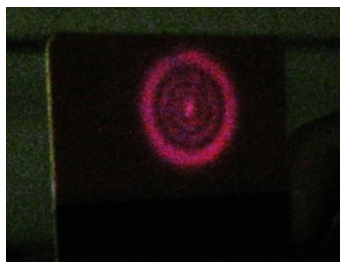


Figure 5: UTLIS0, reference light source located on Nasmyth Table of the UT. Its operation is described in the main text. This image corresponds to a UT on the West Arm of MROI, for which mirror M4 is placed on the NT. This imposes spatial constraints for positioning of the UTLIS optomechanics. For UTs on other arms, M4 is instead housed within the vacuum beam relay pipes.

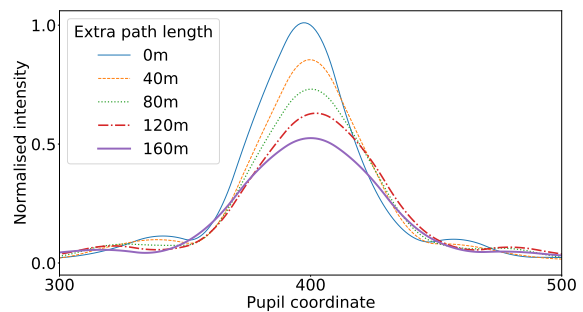
Another downside of a narrower beam is that the pupil arriving at BEASST might be undersampled and so its shear measurement resolution might be degraded. To test, we adapted a beam propagation simulation<sup>3</sup> to generate BEASST0 images in which the beam (Gaussian profile,  $d_{1/e^2} = 32.7\text{mm}$ ) was sheared incrementally. The results suggested that the measurement resolution would be  $\sim 50\ \mu\text{m}$  in 13mm-space. This was thankfully within the requirement of  $65\ \mu\text{m}$ , so we proceeded with deployment of UTLIS0 at MROI. While BEASST0 compresses beam inputs by 4x, the production version will compress by 6x. Therefore it will be sensible to increase the focal length of the collimating optic for UTLIS to achieve a wider beam diameter for BEASST measurements.

### 3.2 Diffraction rings

In laboratory tests, the intensity profile of the collimated beam was measured to be Gaussian about 1 metre away from the lens. By installing UTLIS0 at the UT, we were immediately able to access beam paths that were much longer than were possible in the laboratory. Strangely, we observed diffraction rings in the beam profile after it emerged from the vacuum pipe in the BCA (Fig 6a), which corresponds to a path length of approximately 40 m to 50 m. The phase of the rings varied with distance along the optical axis. Consequently it was difficult to collimate UTLIS0 by the common method of equalising the beam diameter at two planes along its path. After beam compression, the structure smoothed to a central lobe and dimmer sidelobes, but widened as extra path was added by the delay line (Fig 6b). This added difficulties for extracting tilt from BEASST images because our implementation of the pipeline relies on Zernike polynomials defined over a circle of fixed radius.<sup>4,5</sup> In the end these observations were attributed to a small amount of residual spherical aberration induced by the collimating lens,  $\sim \lambda/5$  peak to valley (Fig 7a). Simulations in Zemax reproduced our observations (Fig 7b). We are considering an off-axis parabola for the production version of UTLIS owing to its aspherical surface and achromaticity (two or more wavelengths will serve detectors of differing responses). We are in the process of using Zemax's tolerancing analysis and physical optics propagation to assess the feasibility of this approach.

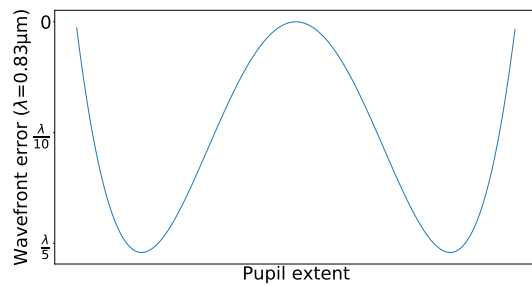


(a) Profile sampled by a viewing card in the BCA in the spacing between the beam relay and delay line pipes. Image credit: Chris Haniff

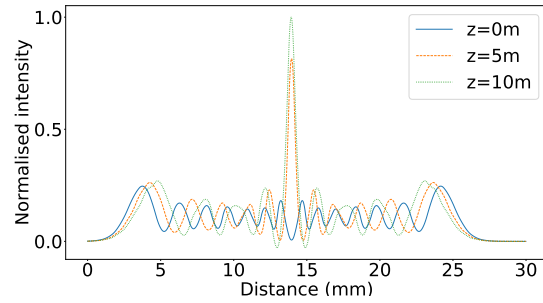


(b) Profile sampled by BEASST0 after 7.3x beam compression. With extra path, achieved by slewing the delay line trolley, the central peak reduced in amplitude and the profile widened.

Figure 6: Observations of UTLIS0 intensity profile



(a) Wavefront error of the collimated UTLIS0 beam at best focus of the lens, obtained by raytracing. The peak to valley error across the aperture is just over  $\lambda/5$ .



(b) Intensity profile as a function of distance between the beam relay and delay line, obtained using physical optics propagation within Zemax.

Figure 7: Results of analysis with Zemax to confirm that spherical aberration caused the observations in Fig 6a

### 3.3 Tilt fluctuation over few second timescale

During a speculative investigation of vibrations, we found evidence that the beamline experiences internal seeing. In the experiment, UTLIS0 was shone down the beam train and measured on BEASST0 at a frame rate of 120Hz for about 10 seconds. A non-periodic fluctuation in tilt was apparent in the UTLIS0 beam over time scales of a few seconds. During human activity in the BCA, its peak-to-peak amplitude was 11" (arcseconds in 13mm-space). It reduced to ~6" when the BCA was uninhabited for 24 hours, and to ~2" when the UT dome was open for observing. For context, the error budget for a tilt measurement by BEASST is <math><0.7''</math>. The fluctuations seem to be induced in the 95mm-space (in the BCA and at the UT enclosure) then amplified by beam compression. The effect of human presence in the BCA should reduce once a vacuum pipe is installed in the path between the beam relay and delay line – they are not currently connected, for convenience. The remaining 2" jitter would lead to longer averaging times when determining the instantaneous tilt and shear of the UTLIS beam. If starlight experiences the same turbulence, fringes formed by two H-band beams would lose contrast by up to 3%. We will attempt to passively mitigate the enclosure's contribution by, for example, blocking air flows near UTLIS0.

#### 4. STARLIGHT IN THE BEAM COMBINING AREA

The prototype alignment equipment enabled us to, for the first time, pass light from a unit telescope through a full beam train to the BCA. This success followed from an alignment procedure that used MOB0, UTLIS0, quad cells and alignment targets. The UTLIS0 beam was shone downstream to arrive at BEASST0 unvignetted. On observing nights the UTLIS0 tilt was set as the fiducial for FTT correction of starlight, so that the beam ejected by the UT should have been parallel to UTLIS0. When the UT was slewed to a star, we immediately observed a signal on BEASST0.

We photographed starlight arriving in the BCA. The images in Figures 8 and 9 were averaged over several seconds to smooth out speckles due to atmospheric seeing. The blue colour originates from a leakiness in the splitter coating for the FTT dichroic, which otherwise prevents visible stellar light from passing to the BCA. Figure 8 shows the UT aperture as viewed from >50 metres along the beamline and captured with a DSLR camera fitted with a telephoto zoom lens.

Figure 9 shows the beam as it appears on the bare sensor of an APS-C format DSLR camera. The beam was ~30% wider than expected, which we suspect was due to a small imperfection in focussing the DL trolley optics. Regardless, we realised that it would be beneficial for the production version of BEASST to feature an oversized clear aperture to accept larger beams – for the longest path lengths of MROI, stellar beam diameters somewhat larger than 13 mm are expected, due to diffraction. More clear aperture would also allow greater shears to be measured before the beam vignettes on BEASST itself.

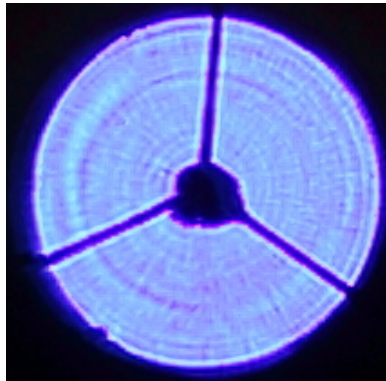


Figure 8: Telescope aperture illuminated by starlight as viewed along the beamline by a DSLR camera with telephoto zoom lens

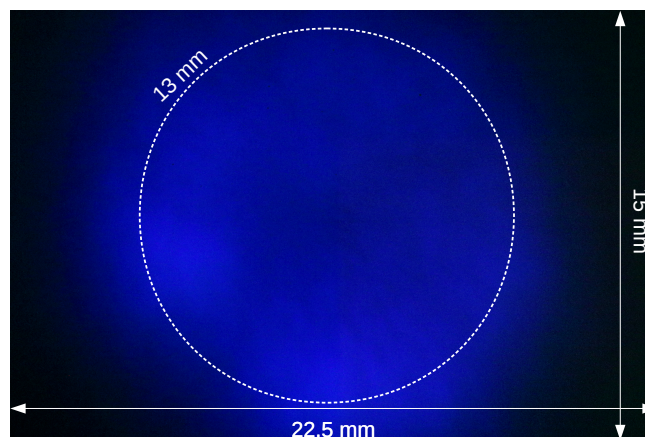
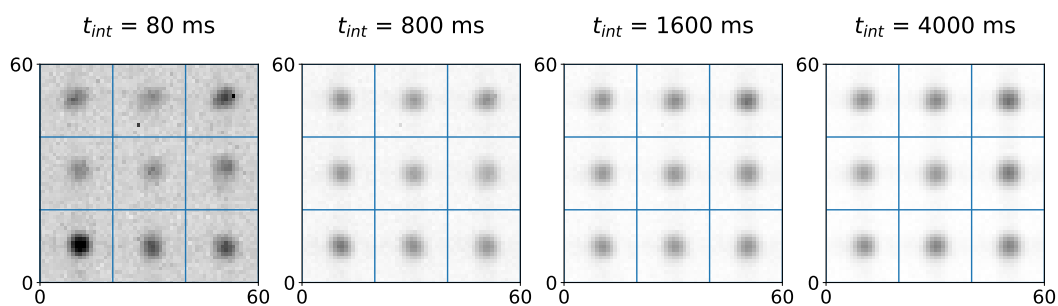


Figure 9: Collimated beam on bare DSLR sensor (APS-C format). The expected 13 mm diameter is marked for comparison.

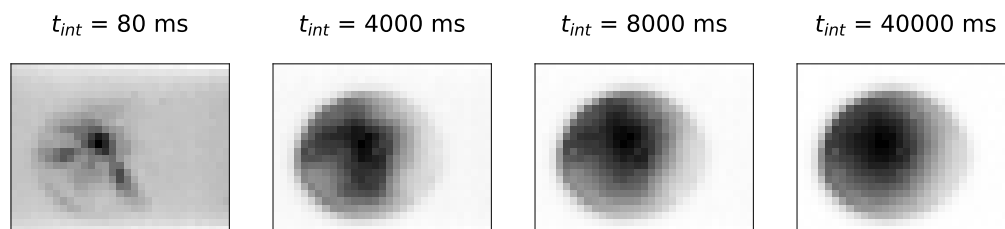
We captured J-band starlight with BEASST0, a Shack-Hartmann sensor that simultaneously measures beam tilt and shear. Tilt is measured from the displacement of the subaperture spots, which encode local wavefront slopes. We reconstruct the wavefront using Zernike polynomials, and extract the low-order components that correspond to average beam tilt. For shear, we sum the signal within subapertures, then reduce the Shack-Hartmann image to one where each pixel is a microlens. This recovers the intensity profile in the pupil plane, from which a centroid is measured.

Atmospheric seeing causes two effects for BEASST images. In the pupil plane, a speckle pattern appears that changes structurally frame by frame. In the image plane, the subaperture spots are displaced by the wavefront corugation resulting from transmission through the atmosphere. If the slopes change on a timescale that is faster than the camera exposure time, then motion blur appears to distort the spots. In both the pupil and image plane, centroid accuracy is reduced and the resulting shear and tilt measurements exceed the error budget by large factors. BEASST must average consecutive frames to recover centroid accuracy. We found that subaperture spots smooth quickly (Figure 10a), while the pupil smooths slowly (Figure 10b). Note, however, that the seeing conditions during these measurements have not yet been estimated.

A smooth stellar pupil is needed for calibrating its shear offset relative to UTLIS once per hour; a long exposure time would be acceptable in this case. For bright targets ( $m_H < 4$ ) we hope to use starlight to iteratively sample beam alignment for intra-night correction, every  $\sim 10$  mins; here, long exposures are unfeasible. To tackle the problem we will use existing data to attempt pupil correlation for centroid estimation, which might be more tolerant of speckle than the current thresholded centre-of-mass method. When facility operations can resume, we will collect more on-sky BEASST0 images to understand the impact of different seeing conditions.



(a) Subset of BEASST0 microlens spots. Coordinates are in camera pixels. Distorted and offset spots smooth out within just a few exposures.



(b) Reconstructed pupil using BEASST0 images. Each pixel represents one microlens of the Shack-Hartmann array. Speckles are obvious in short exposures and smooth slowly with additional integration.

Figure 10: Averaging of BEASST0 images with varying integration time  $t_{int}$ .

## 5. SOFTWARE

During the commissioning run, we generally controlled hardware by running low-level applications on computers that were local to the devices. Operations would have been simpler if the software had been unified. In 2020 we prioritised development of the AAS software architecture to begin tying applications together into a coherent system.

The AAS must manage alignment tasks within the framework of the Interferometer Supervisory System (ISS)<sup>6</sup> that provides the software interface between all subsystems. Unlike most other subsystems of MROI, the AAS hardware is distributed among several locations along every telescope beam line. Our goal is to directly control all hardware for a single beamline using an application running on one computer. For example, to adjust the brightness of a light source, we use a networked digital-to-analog converter that accepts commands from a remote computer. We will also employ RS232 and USB device servers, which make remote devices appear as if they are local resources for the computer.

We define three distinct software components:

- AAS Beam Train Controller (ABTC) – directly interacts with the hardware components, such as light sources and cameras. One instance of ABTC will execute per beamline.
- AAS Umbrella System (AUS) – coordinates alignment tasks for all ten beamlines of the interferometer. It will monitor the alignment status of each beamline and manage scheduling in case two or more beamlines are making conflicting requests to use shared hardware, such as a common light source.
- AAS GUI – allows a human operator to view the status of alignment tasks and to take control for troubleshooting if a task fails. This application can be run on several computers at a time to allow multiple human operators to work in parallel.

We have tested protocols for interaction between applications running within the ISS framework. In future work we will roll separate hardware applications into ABTC.

In addition to the architecture, we have made progress on implementing some hardware control routines. One major milestone was the development of an application to operate the Raptor Owl 640 camera of BEASST via Gigabit Ethernet (GigE). The camera's built-in communication interface is CameraLink (CL), which requires a direct connection between the camera and a PCIe frame grabber installed in a computer. Since BEASST will be operated in a thermally

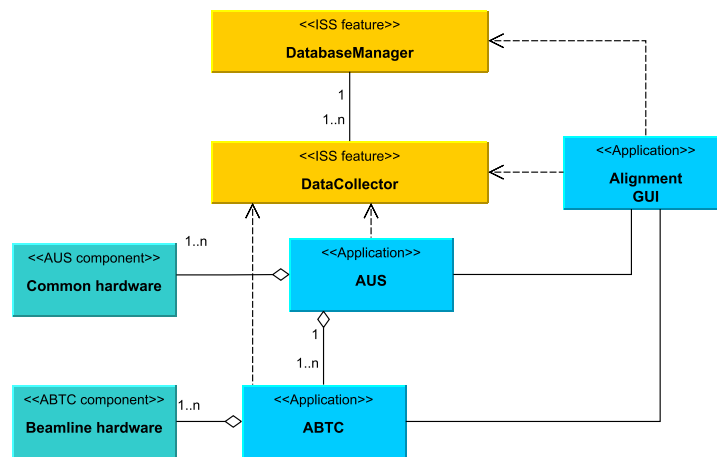


Figure 11: Software architecture for the AAS. AUS, ABTC and Alignment GUI form the skeleton of the architecture. The boxes "common hardware" and "beamline hardware" indicate the low level software that controls hardware – they will run within the AUS and ABTC applications respectively. The AAS will use the ISS framework for data collection and database access. Although not represented here, the AAS will interact directly with other subsystems of MROI using ISS communication protocols.

stable environment, we want to avoid installing a heat-producing computer in the vicinity. We briefly considered running the CL cable out of the room, but encountered performance issues when it was longer than 5m. Our chosen solution is to connect the camera to a Pleora iPort CL-GigE frame grabber that reads images and streams them over the GigE network, and additionally provides an interface for configuring exposure settings. In principle, any computer on the network can view the images. It will be trivial to multiplex additional BEASST cameras as more beamlines become available. Our implementation is based on C++/Qt. We are now able not only to stream images, but to measure beam alignment parameters in close to real time. Currently tilt and shear extraction repeats at about 1 Hz. The bottleneck is caused by calls from the C++ program to a python library that implements the pipeline for reducing images. We are in the process of porting this pipeline to C++ so that it can run natively within the application.

## 6. CONCLUSION AND FUTURE PLANS

The findings outlined in this paper have prompted us to update the design of some aspects of the AAS. In particular, we will pivot to using an off-axis parabola as the collimating optic for UTLIS (to sidestep the effect of spherical aberration), and we will increase the clear aperture for BEASST (to accommodate larger beams and greater dynamic range in shear). We must also investigate some issues which we do not fully understand yet, such as the tilt fluctuations imposed on UTLIS0 at the Nasmyth Table and the performance of BEASST shear measurements when observing starlight under different seeing conditions. We do not expect to make progress on these investigations until mid 2021 while we await a return to regular operations at the interferometer.

The Final Design Review (FDR) for the AAS hardware will be held in the next few months. Some outstanding work remains in addition to the issues described above. The optomechanical designs for UTLIS, BEASST and MOB have progressed significantly from the preliminary design presented at the SPIE meeting in 2018<sup>7</sup> but must be finalised and costed. Once the design has passed FDR, we intend to purchase, assemble and validate production units for two beamlines, in support of our goal of achieving first stellar fringes.

We will also make a push on developing software for the AAS, which will not be hindered by the facility shutdown. Low level control applications exist in some form for the vast majority of the AAS, but must be fitted together into a single application. After this is complete, the next step would be to develop a GUI for human interaction. Finally we will write and test the algorithms for automating the start-of-night and intra-night procedures.

## ACKNOWLEDGMENTS

This material is based on research sponsored by Air Force Research Laboratory (AFRL) under agreement number FA9453-15-2-0086. The U.S. Government is authorized to reproduce and distribute reprints for Governmental purposes notwithstanding any copyright notation thereon. The views and conclusions contained herein are those of the authors and should not be interpreted as necessarily representing the official policies or endorsements, either expressed or implied, of Air Force Research Laboratory (AFRL) and/or the U.S. Government. The work has also been partially supported by a Science & Technology Facilities Council studentship.

## REFERENCES

- [1] Buscher, D. F., [*Practical Optical Interferometry*], Cambridge University Press, Cambridge, UK (2015).
- [2] Young, J. et al., "The MROI fast tip-tilt correction and target acquisition system," *SPIE Proceedings of Optical and Infrared Interferometry III* **8445** (2012).
- [3] A. J. Horton, D. F. B. and Haniff, C. A., "Diffraction losses in ground based optical interferometers," *MNRAS* **327**, 217–226 (2001).
- [4] Tyson, R. K., [*Principles of Adaptive Optics*], CRC Press, Boca Raton, FL, USA (2011 (Third Edition)).
- [5] Stephenson, P. C. L., "Recurrence relations for the Cartesian derivatives of the Zernike polynomials," *J. Opt. Sci. Am. A* **31**(4) (2014).
- [6] Farris, A. et al., "Implementing the Magdalena Ridge Observatory Interferometer supervisory system," *SPIE Proceedings of Software and Cyberinfrastructure for Astronomy V* **10707** (2018).
- [7] Luis, J. J. D. et al., "Augmented design for a fully automated alignment system at the Magdalena Ridge Observatory Interferometer," *SPIE Proceedings of Optical and Infrared Interferometry VI* **10701** (2018).